USGS award number G10AP00060

Title: Improving thermal models for the Cascadia subduction zone by including hydrothermal circulation in subducting crust

Glenn A. Spinelli
Earth & Environmental Science Department, New Mexico Institute of Mining and Technology, Socorro, NM, USA

Award term: March 15, 2010 – September 14, 2011

Publications resulting from this work:
Cozzens, B.D., and Spinelli, G.A., submitted, A wider seismogenic zone at Cascadia due to fluid circulation in subducting oceanic crust, *Geology.*

Abstract

We have developed new thermal models for the Cascadia subduction zone that include the effects of fluid flow in the subducting crust. On the Cascadia margin, temperatures along the subduction zone plate boundary fault have been used to estimate the area and extent of the seismogenic zone. The extent of the Cascadia seismogenic zone is poorly resolved due to the lack of a large megathrust event during the instrumental record, but rock friction experiments indicate a seismogenic zone between 150 and 350 ˚C. Our thermal models that are most consistent with both surface heat flux measurements and slab alteration observations include fluid circulation in an ocean crust aquifer with permeability ~10^{-10} m^2. This fluid circulation cools the subduction zone and widens the thermally-defined seismogenic zone by shifting the intersection of 350°C with the plate boundary fault ~30-55 km landward. This wider seismogenic zone is consistent with recent models of interseismic deformation.

Introduction

Thermally-controlled alteration of sediment and rock links changes in physical properties and temperatures along subduction zone plate boundary faults (Hyndman and Wang, 1993; Blanpied et al., 1995). The seismogenic portion of a subduction megathrust likely extends from 150 to 350 ˚C (Hyndman and Wang, 1993; Hyndman et al., 1995). The updip limit of seismicity is suggested to result from a host of diagenetic processes triggered at ~100-150 ˚C (Moore and Saffer, 2001). The downdip limit of seismicity is posited to occur at a transition from velocity-weakening to velocity-strengthening behavior at ~350 ˚C (Hyndman and Wang, 1993; Blanpied et al., 1995), or at the intersection of the plate boundary fault and the continental Mohorovicic discontinuity if it occurs at <350 ˚C (e.g., Oleskevich et al., 1999). Thermal models for the Cascadia margin constrained by surface heat flux data have been applied to estimate the extent of the seismogenic zone (Fig. 1). However, due to the dearth of instrumentally recorded megathrust earthquakes in the Cascadia subduction zone, verification of the constraints on the seismogenic zone provided by these original thermal models (Hyndman and Wang, 1993) is difficult.

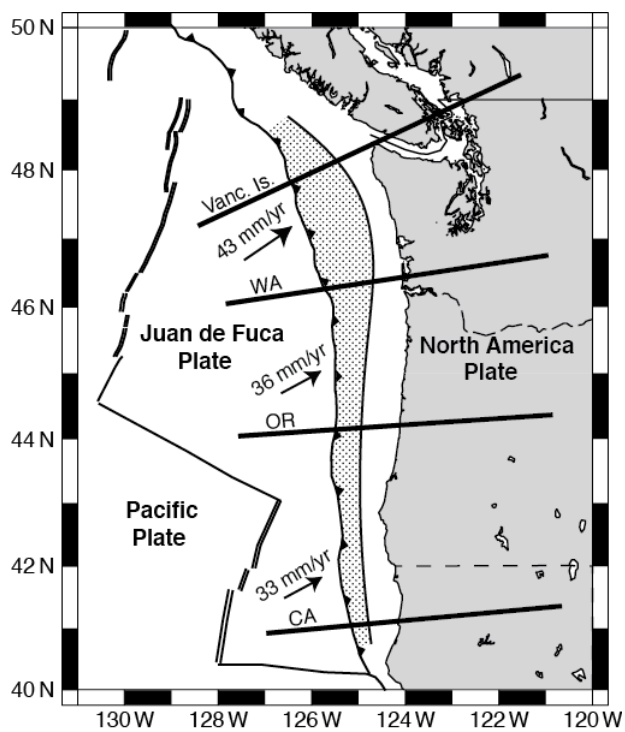

Figure 1: Map of the Cascadia subduction zone showing plate boundaries, the locations of four thermal model transects for this study, and the previously defined Cascadia megathrust seismogenic zone (stippled; Hyndman and Wang, 1993). Arrows are convergence vectors along the margin.

Studies of the well-constrained Nankai margin of southern Japan show that the seismogenic portion of the

plate boundary fault is between the key temperatures of 150 and 350 ˚C, and that hydrothermal circulation in the subducting crust cools the subduction zone, widening the 150–350 ˚C portion of the plate boundary fault (Spinelli and Wang, 2008). For both the Nankai margin and the subduction zone offshore Costa Rica, thermal models that include the effects of fluid circulation in the subducting crust are most consistent with observed surface heat flux anomalies (Spinelli and Wang, 2008; Harris et al., 2010). Vigorous hydrothermal circulation in the high-permeability upper ~600 m of basalt in the oceanic crust (i.e. the basement aquifer of oceanic crust) transports heat laterally (Davis et al., 1997). This is buoyancy driven circulation of seawater that enters the basement aquifer at basaltic outcrops; fluid sources in the oceanic crust, including dehydration reactions in the slab, are small (Peacock, 1996). Far from outcrops, fluid circulation persists in the sediment-covered aquifer; observations in the crust approaching the Cascadia subduction zone indicate that the oceanic crust aquifer is continuous over 10's of km, with fluid flow velocities of 100's to 1000's of m yr^{-1} (Fisher et al., 2003). In a warm subduction zone the width of convection cells in the basement aquifer is controlled by aquifer topography (Kummer and Spinelli, 2009). Thus, wide convection cells mine heat from the subducted crust and transport it updip in the aquifer to the incoming plate. We develop new thermal models for the Cascadia subduction zone that include the effects of fluid circulation in the subducting crust. We use both surface heat flux data and the location of the basalt-to-eclogite transition in the subducting crust to constrain the thermal models. These thermal models yield a new estimate for the potential rupture area for a Cascadia megathrust earthquake.

Numerical modeling method

To estimate temperatures in the Cascadia subduction zone, we use a 2-D finite element heat transfer model (Hyndman and Wang, 1993; Curry et al., 2004). The thermal model accounts for heat production by plate boundary fault friction and radioactive decay, and for heat transport by conduction, advection of the subducting slab, mantle wedge flow, and vigorous fluid circulation in an oceanic crust aquifer (Spinelli and Wang, 2008). We use a conductive proxy to simulate the thermal effects of fluid circulation in the oceanic crust aquifer (Davis et al., 1997; Spinelli and Wang, 2008). In this approach, a Rayleigh number (*Ra*) is defined for each aquifer element using the permeability, temperature-dependent fluid density and viscosity, and local heat flux. An elemental Nusselt number (*Nu*), which quantifies the local efficiency of convective heat transfer, is derived from *Ra* using an empirical *Ra*-*Nu* relationship. Multiplying the thermal conductivity by *Nu* then simulates the thermal effects of hydrothermal circulation. Additional details of the modeling method are provided in Supplementary Material. We model subduction zone temperatures with and without fluid circulation in the aquifer. For the simulations with fluid circulation, we explore a range of aquifer permeabilities. In all cases aquifer permeability decreases with burial depth, simulating the chemical and mechanical sealing of fractures as the ocean crust is progressively altered and compacted throughout subduction. We run simulations with pre-subduction aquifer permeability of 10^{-10}, $2x10^{-10}$, and 10^{-9} m^2, spanning the range of estimates for regional-scale ocean crust permeability (Becker and Davis, 2004).

For each of the four transects examined (Fig. 1), the geometry of the subduction zone is constrained by seismic reflection and refraction data, earthquake hypocenters, and teleseismic travel-time data (Fuis, 1998; Gerdom et al., 2000; Flueh et al., 1998; Gullick et al., 1998; McCrory et al., 2006). Surface heat flux observations provide the primary constraint for most subduction zone thermal models. In addition to those data (Hyndman and Wang, 1993; Hyndman and Wang, 1995; Trehu, 2006; Booth-Rea et al., 2008), we use the seismically observed location of the basalt-to-eclogite transition in the subducting crust to constrain our thermal models. In the Cascadia margin, inversion of scattered teleseismic body waves indicates a dipping layer 5-9 km thick with velocities 5-15% slower than the surrounding material, interpreted as the subducting crust (Nicholson et al., 2005; Abers et al., 2009; Rondenay et al., 2008). The disappearance of this low velocity layer farther into the subduction zone occurs at the basalt-to-eclogite transition; once converted to eclogite, the oceanic crustal rocks are seismically indistinguishable from the surrounding mantle. We determine the pressure-temperature (P-T) conditions at the center of the subducting basaltic crust (3 km below the top of the subducting basement rock) under various hydrologic conditions. We use a phase diagram for mid-ocean ridge basalt (Hacker et al., 2003) and the modeled P-T conditions to determine the depth at which the modeled subducting crust experiences eclogite metamorphism. These results are compared with the depths at which the center of the observed low velocity layer disappears.

Results

In the regions with most of the surface heat flux observations, on the incoming plate and margin wedge within ~40 km of the trench, modeled surface heat flux provides little to discriminate among many of the scenarios examined (Fig. 2). For the Oregon, Washington,

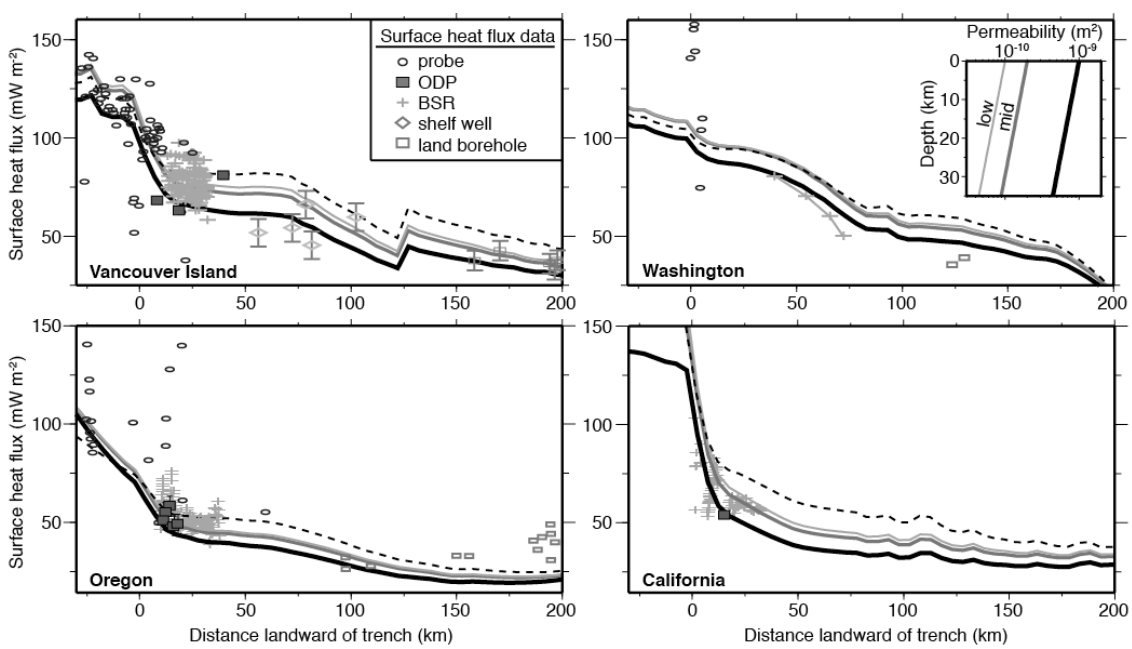

Figure 2: Measured and modeled surface heat flux along the four transects shown in figure 1. Dashed lines are modeled heat flux with no fluid circulation in the ocean crust. Solid lines are modeled surface heat flux with fluid circulation; inset shows oceanic crust permeability trends, line weights and shading are keyed to model results.

and Vancouver Island transects, modeled heat flux in all of the scenarios examined passes through the scattered data; the scatter in the data may reflect local advection and/or venting of fluid and heat. In these transects, the surface heat flux drops gradually moving landward across the trench; in contrast, the landward drop in surface heat flux near the trench is much steeper in the California transect. This difference results from geometric differences, particularly thicker sediment in the northern Cascadia subduction zone than in the California transect. For the California transect, models with fluid circulation are more consistent with the observed surface heat flux than a model with no fluid circulation; however, each of the three models with different permeability trends reasonably approximates the data, with little to discriminate between them. Because comparison of the modeled and observed surface heat flux is largely equivocal, the location of the basalt-to-eclogite transition for the subducting crust is a critical constraint on the thermal state of the Cascadia margin.

Subduction of hydrothermally cooled crust shifts the basalt-to-eclogite transition farther landward than would be predicted with no fluid flow, for all but the hottest (i.e. California) transect (Table 1). Hydrothermal cooling shifts the modeled basalt-to-eclogite transition seaward in the California transect because the P-T path in the no fluid flow case enters the eclogite field across a phase boundary with a positive Clapeyron slope. Seismic velocity anomalies indicate the transition from hydrated basaltic crust to eclogitized material at ~45 km depth for the Vancouver Island, Washington, and Oregon transects (Nicholson et al., 2005; Rondenay et al., 2008; Abers et al., 2009); similar data are not available for the California transect. For the Vancouver and Washington transects, models with fluid circulation are more consistent with the observed basalt-to-eclogite transition than models without fluid flow (Fig. 3). In selecting preferred thermal models for each transect, we choose the warmest (i.e. lowest permeability, least hydrothermally cooled) scenario for each transect consistent with the seismically observed basalt-to-eclogite transition location (Fig.

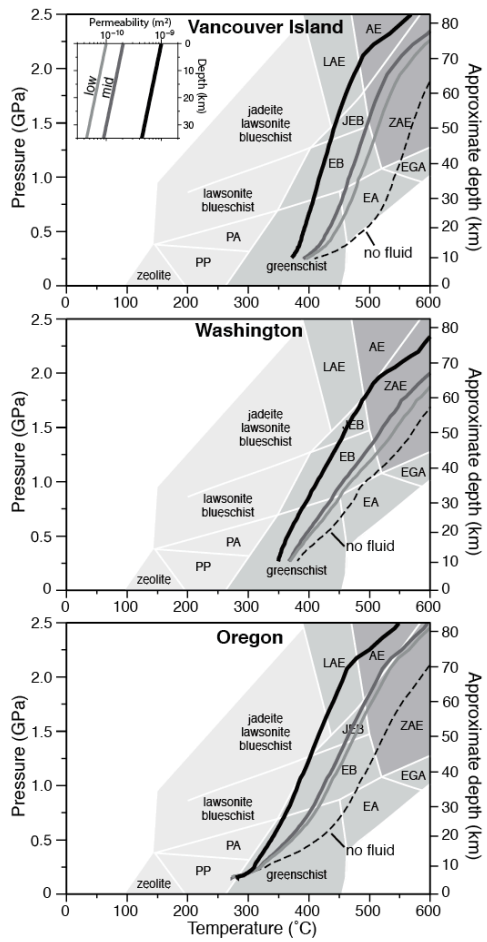

Figure 3: Pressure-temperature (P-T) paths for the center of the subducting crust (3 km below top of basaltic basement rock). These paths are overlain on a phase diagram showing metamorphic facies for mid-ocean ridge basalt (Hacker et al., 2003). We compare the location at which the modeled P-T paths enter the eclogite facies (ZAE or AE) to the seismically observed location of crust eclogitization. Dashed lines are from models with no fluid circulation. Darker shading indicates lower water content in oceanic crust.

4) and the surface heat flux observations. Thus, we use the models with the lowest permeability ocean crust for Vancouver Island, Washington, and California transects; we use the no fluid flow model for the Oregon transect. This yields a conservative (i.e. smallest) thermally-defined seismogenic zone for the Cascadia subduction zone that extends ~30-55 km farther landward than earlier estimates, with the downdip limit of seismicity under the coastline along Washington (Fig. 5).

Table 1: Depth (km) to modeled basalt-to-eclogite transition for subducting crust

Transect	No fluid flow	Low permeability	Intermediate permeability
Vancouver	41	46	52
Washington	40	44	47
Oregon	45	56	59
California	49	40	42

For the preferred models, the permeability of the subducting ocean crust aquifer (and therefore the vigor of hydrothermal circulation) is lower than estimated for either the Nankai (Spinelli and Wang, 2008) or Costa Rica (Harris et al., 2010) margins. This difference may result from regional-scale permeability anisotropy for the ocean crust aquifer, with structurally-controlled high permeability parallel to the mid-ocean ridge axis (Fisher et al., 2008). On the Nankai and Costa Rica margins, magnetic lineations in the ocean crust are nearly perpendicular to the trench (Okino et al., 1994; Barckhausen et al., 2001). This orientation of the high permeability direction in the ocean crust aquifer could facilitate hydrothermal circulation exchanging heat between the subducted and incoming ocean crust (Harris et al., 2010). Magnetic lineations for the incoming plate on the Cascadia margin are oblique to the trench offshore Vancouver Island; they transition to sub-parallel to the trench offshore Oregon (Wilson, 1993). This is consistent with less hydrothermal heat extraction from the subducted crust for the Cascadia margin than for Nankai or Costa

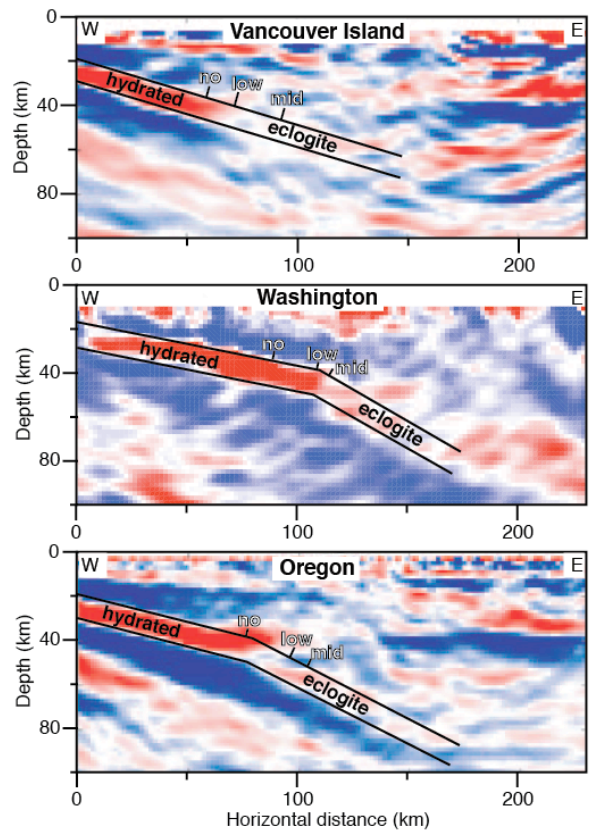

Figure 4: Scattered wave inversion cross-sections for Vancouver Island (Nicholson et al., 2005), Washington (Abers et al., 2009), and Oregon transects (Rondenay et al., 2008). Red indicates slow S-wave velocity; blue indicates fast S-wave velocity (range is ±10% relative to a background model for Vancouver Island and Oregon, ±5% for Washington). The locations at which the slab is expected to undergo eclogitization for thermal models with no fluid flow and hydrothermal circulation in ocean crust with the low and intermediate permeability trends (Figure 2 inset) are indicated by ticks labeled no, low, and mid, respectively.

Rica. In addition, this could explain why there may be less hydrothermal cooling for the Oregon transect than for Vancouver Island and Washington transects. Subduction of older ocean crust offshore Oregon (~9 Ma) than offshore Vancouver Island (~7 Ma) may also limit the effect of hydrothermal cooling in the Oregon transect, given a trend for decreasing ocean crust aquifer permeability with increasing crustal age (Becker and Davis, 2004). Our temperature estimates for the Oregon transect are slightly lower than previous estimates (Hyndman and Wang, 1993) due to our use of updated margin geometry and convergence rate data; this temperature difference is small relative to the large shifts due to hydrothermal cooling for the Vancouver Island and Washington transects (Fig. 5).

The downdip edge of the thermally-defined seismogenic zone is within ~60 km of the region of episodic tremor and slip (ETS) in the Vancouver Island, Washington, and Oregon transects, and within ~80 km of the ETS region in southern Cascadia (Wech and Creager, 2011). For Vancouver Island, Washington, and Oregon, our thermal estimates indicate temperatures on the plate boundary fault at the updip end of the ETS region ~410 ˚C; temperatures at the downdip end are 500 – 550 ˚C. In the California transect, where younger (~5 Ma) warmer lithosphere is subducting, the plate interface in the ETS region is warmer, ~480 - 575 ˚C.

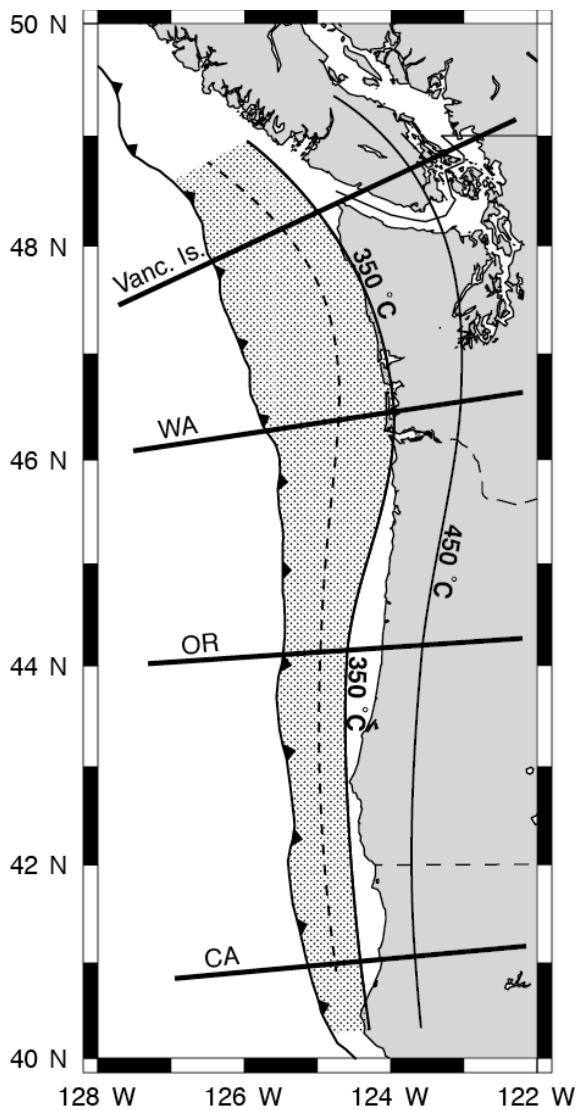

Figure 5: Map of Cascadia subduction zone with probable megathrust seismogenic zone, portion of plate boundary fault from 150-350 ˚C, stippled. The seismogenic zone extends up to 55 km farther landward than previously estimated (dashed line), including under the coastline of Washington.

Conclusions

New thermal models for the Cascadia margin consistent with surface heat flux data and the observed locations of subducting crust alteration indicate that hydrothermal circulation cools the subduction zone and widens the portion of the plate boundary fault between 150 and 350 ˚C. The location and extent of this thermally-defined seismogenic zone is consistent with the distribution of interseismic locking on the plate interface (Chapman and Melbourne, 2009; McCaffrey, 2009). The location of the basalt-to-eclogite transition in the subducting crust provides an important constraint on thermal models for the

margin because hydrothermal circulation in the oceanic crust aquifer produces only small surface heat flux anomalies on this margin with thick sediment in the trench and on the incoming plate.

References

Abers, G.A., MacKenzie, L.S., Rondenay, S., Zhang, Z., Wech, A.G., and Creager, K.C., 2009, Imaging the source region of Cascadia tremor and intermediate-depth earthquakes: Geology, v. 37, p. 1119-1122.

Barckhausen, U., Ranero, C.R., von Huene, R., Cande, S.C., and Roeser, H.A., 2001, Revised tectonic boundaries in the Cocos Plate off Costa Rica: Implications for the segmentation of the convergent margin and for plate tectonic models: J. Geophys. Res., v. 106 (B9), p. 19207-19220.

Becker, K., and Davis, E.E., 2004, In situ determinations of the permeability of igneous ocean crust, *in* Davis, E.E., and Elderfield, H., eds., Hydrogeology of the Ocean Lithosphere, Cambridge University Press, p. 189-224.

Blanpied, M.L., Lockner, D.A., and Byerlee, J.D., 1995, Frictional slip of granite at hydrothermal conditions: J. Geophys. Res., v. 100, p. 13045-13064.

Booth-Rea, G., Klaeschen, D., Grevemeyer, I., and Reston, T., 2008, Heterogeneous deformation in the Cascadia convergent margin and its relation to thermal gradient (Washington, NW USA): Tectonics, v. 27, TC4005.

Chapman, J.S., and Melbourne, T.I., 2009, Future Cascadia megathrust rupture delineated by episodic tremor and slip: Geophys. Res. Lett., v. 36, L22301.

Curry, C.A., Wang, K., Hyndman, R.D., and He. J., 2004, The thermal effects of steady-state slab-driven mantle flow above a subducting plate: the Cascadia subduction zone and backarc: Earth Planet. Sci. Lett., v. 223, p. 35-48.

Davis, E.E., Wang, K., He, J., Chapman, D., Villinger, H., and Rosenberger, A., 1997, An unequivocal case for high Nusselt number hydrothermal convection in sediment-buried igneous oceanic crust: Earth Planet. Science Lett., v. 146, p. 137–150.

Fisher, A.T., Davis, E.E., and Becker, K., 2008 Borehole-to-borehole hydrologic response across 2.4 km in the upper oceanic crust: Implications for crustal-scale properties: J. Geophys. Res., v. 113, B07106.

Fisher, A. T., E. E. Davis, M. Hutnak, V. Spiess, L. Zühlsdorff, A. Cherkaoui, L. Christiansen, K. M. Edwards, R. Macdonald, H. Villinger, M. Mottl, C. G. Wheat, and K. Becker, 2003, Hydrothermal circulation across 50 km on a young ridge flank: the role of seamounts in guiding recharge and discharge at a crustal scale, *Nature, 421*, 618-621.

Flueh, E.R., et al., 1998, New seismic images of the Cascadia subduction zone from cruise SO108 – ORWELL: Tectonophysics, v. 293, p. 69-84.

Fuis, G.S., 1998, West margin of North America – a synthesis of recent seismic transects: Tectonophys., v. 288, p. 265-292.

Gerdom, M., Trehu, A.M., Flueh, E.R., and Klaeschen, D., 2000, The continental margin off Oregon from seismic investigations: *Tectonophysics, v.* **329**, p. 79-97.

Gullick, S.P.S., Meltzer, A.M., and Clarke Jr., S.H., 1998, Seismic structure of the southern Cascadia subduction zone and accretionary prism north of the Mendocino triple junction: J. Geophys. Res., v. 103, p. 27207-27222.

Hacker, B.R., Abers, G.A., and Peacock, S.M., 2003, Subduction factory 1. Theoretical mineralogy, densities, seismic wave speeds, and H2O contents: J. Geophys. Res., v. 108, 2029, doi:10.1029/2001JB001127.

Harris, R.N., Spinelli, G., Ranero, C.R., Grevemeyer, I., Villinger, H., and Barckhausen, U., 2010, Thermal regime of the Costa Rican convergent margin: 2. Thermal models of the shallow Middle America subduction zone offshore Costa Rica: Geochem. Geophys. Geosys., v. 11, Q12S29.

Hyndman, R.D., and Wang, K., 1993, Thermal constraints on the zone of major thrust earthquakes failure: The Cascadia subduction zone: J. Geophys. Res., v. 98, p. 2039-2060.

Hyndman, R.D., and Wang, K., 1995, The rupture zone of Cascadia great earthquakes from current deformation and the thermal regime: J. Geophys. Res., v. 100, p. 22133-22154.

Hyndman, R.D., Wang, K., Yamano, M., 1995, Thermal constraints on the seismogenic portion of the southwestern Japan subduction thrust: J. Geophys. Res., v. 100, p. 15373-15392.

Kummer, T.D., and Spinelli, G.A., 2009, Thermal effects of fluid circulation in the basement aquifer of subducting ocean crust: J. Geophys. Res., v. 114, B03104, doi:10.1029/2008JB006197.

McCaffrey, R., 2009, Time-dependent inversion of three-component continuous GPS for steady and transient sources in northern Cascadia: Geophys. Res. Lett., v. 36, L07304.

McCrory, P.A., Blair, J.L., Oppenheimer, D.H., and Walter, S.R., Depth to the Juan de Fuca Slab Beneath the Cascadia Subduction Margin—A 3-D Model for Sorting Earthquakes: USGS Data Series 91.

Moore, J.C., and Saffer, D., 2001, Updip limit of the seismogenic zone beneath the accretionary prism of Southwest Japan: An effect of diagenetic to low-grade metamorphic processes and increasing effective stress: *Geology*, v. **29**, p. 183-186.

Nicholson, T., Bostock, M.G., and Cassidy, J.F., 2005, New constraints on subduction zone structure in northern Cascadia: Geophys. J. Int., v. 161, p. 849-859.

Okino, K., Shimakawa, Y., and Nagaoka, S., 1994, Evolution of the Shikoku Basin: J. Geomag. Geoelectr., v. 46, p. 463-479.

Oleskevich, D.A., Hyndman, R.D., and Wang, K., 1999, The updip and downdip limits of great subduction earthquakes: Thermal and structural models of Cascadia, south Alaska, SW Japan, and Chile: J. Geophys. Res. v. 104, p. 14965-14991.

Peacock, S.M., 1996, Thermal and petrologic structure of subduction zones, in *Subduction: Top to Bottom, Geophys. Monogr. Ser., 96*, edited by G. E. Bebout et al., pp. 119-133, AGU, Washington, D.C..

Rondenay, S., Abers, G.A., and van Keken, P.E., 2008, Seismic imaging of subduction zone metamorphism: Geology, v. 36, p. 275-278.

Spinelli, G.A., and Wang, K., 2008, Effects of fluid circulation in subducting crust on Nankai margin seismogenic zone temperatures: Geology, v. 36, p. 887-890.

Trehu, A., 2006, Subsurface temperatures beneath southern Hydrate Ridge: Proc. Ocean Drilling Prog. Sci. Res., v. 204, p. 1-26.

Wech, A.G., and Creager, K.C., 2011, A continuum of stress, strength, and slip in the Cascadia subduction zone: Nature Geoscience, v. 4, p. 624-628.

Wilson, D. S., 1993, Confidence intervals for motion and deformation of the Juan de Fuca Plate: J. Geophys. Res., v. 98, p. 16053-16071.